Journal of Power Sources 185 (2008) 136–142

Contents lists available at ScienceDirect

Journal of Power Sources

journal homepage: www.elsevier.com/locate/jpowsour

Improvement of the proton exchange membrane fuel cell (PEMFC) performance at low-humidity conditions by adding hygroscopic γ-Al_2O_3 particles into the catalyst layer

Wen-Kai Chao[a], Chih-Ming Lee[a], Du-Cheng Tsai[a], Chih-Cheng Chou[b], Kan-Lin Hsueh[c], Fuh-Sheng Shieu[a,*]

[a] Department of Materials Science and Engineering, National Chung Hsing University, Taichung 40227, Taiwan
[b] Department of Chemical Engineering, National Chung Hsing University, Taichung 40227, Taiwan
[c] Department of Energy and Resources, National United University, Miaoli 36003, Taiwan

ARTICLE INFO

Article history:
Received 12 March 2008
Received in revised form 10 June 2008
Accepted 10 June 2008
Available online 27 June 2008

Keywords:
Water management
PEMFC
γ-Alumina
MEA

ABSTRACT

In this study, hygroscopic γ-alumina particles were added into the catalyst layer of membrane electrode assemblies (MEAs) to improve the wettability and performance of PEMFC at low-humidity conditions. Hygroscopic γ-alumina particles with a BET surface area of 442 $m^2 g^{-1}$ and an average pore diameter of 9 nm were synthesized by a three-step sol–gel procedure. Uniform Pt/C/γ-alumina catalyst ink was prepared by utilizing an ultrasonic method, and then sprayed on commercial hydrophobic carbon clothes to serve as the catalyst layer. The water contact angles of the catalyst layer with various amounts of γ-alumina additions 0%, 10%, 20% and 40% were measured to be 136°, 109°, 79° and 0°, respectively. Effect of adding γ-alumina particles into the catalyst layer on the single cell performance was investigated under different temperatures of the electrode humidifier. The increased wettability of the cathode catalyst layer with γ-alumina addition reduced the cell performance due to water flooding, which demonstrates the hygroscopic characteristic of γ-alumina particles. On the other hand, when the γ-alumina particles were added into the anode catalyst layer, it was found that the MEA with 10% γ-alumina addition had the highest current density at anode humidifier temperatures ranging from 25 to 55 °C. Nevertheless, the MEA with 40% γ-alumina addition into the anode catalyst layer showed the lowest current density because of the high electrical resistance of the catalyst layer and the water flooding in the anode caused by excess water absorption. The increased wettability of the anode catalyst layer by an appropriate amount of γ-alumina additions also enhances the water adsorption of the anode due to back diffusion.

1. Introduction

Hydrogen is regarded as the best and highly potential clean fuel resource for the future. Proton exchange membrane fuel cells (PEMFCs) using hydrogen and oxygen as reactants are expected to be applied widely in transportation, residence and portable devices in the next decade, providing a clean and friendly environment. This is attributed to their high energy conversion efficiency, high power density, simplicity of operation and near-zero pollutant emission, compared with conventional combustion systems using fossil fuels [1–3]. Nafion® membrane, a key component of membrane the electrode assembly (MEA), is still the most commonly used commercial membrane in PEMFCs nowadays owing to its good chemical, physical and thermal stabilities with high proton conductivity. Since the proton conductivity of the Nafion® membrane relies on the dissociation of protons from the constituent SO_3H groups in the presence of water, the membrane needs to be properly hydrated by a humidifying system to retain an optimum hydration level [4–9]. Low humidity at the anode limits the operation temperature of PEMFCs under 80 °C. Nevertheless, excess humidifying system increases the complexity of the PEMFC structure. In addition, CO-poisoning usually causes a decrease in the activity of Pt in the anode catalyst layer during operation of the PEMFCs at low temperature [10–13]. To solve these problems, a versatile membrane material capable of maintaining optimum hydration level at high temperatures under low humidity conditions is necessary.

Recently, considerable research efforts have been devoted to develop high wettability membrane operated under low-humidity conditions. One of the effective approaches is to prepare organic–inorganic composite membrane by incorporation of hygroscopic metal oxide particles such as ZrO_2, SiO_2 and TiO_2 into Nafion® resin, which can keep appropriate hydration level in the

* Corresponding author. Tel.: +886 4 2285 4563; fax: +886 4 2285 7017.
E-mail address: fsshieu@dragon.nchu.edu.tw (F.-S. Shieu).

0378-7753/$ – see front matter © 2008 Elsevier B.V. All rights reserved.
doi:10.1016/j.jpowsour.2008.06.052

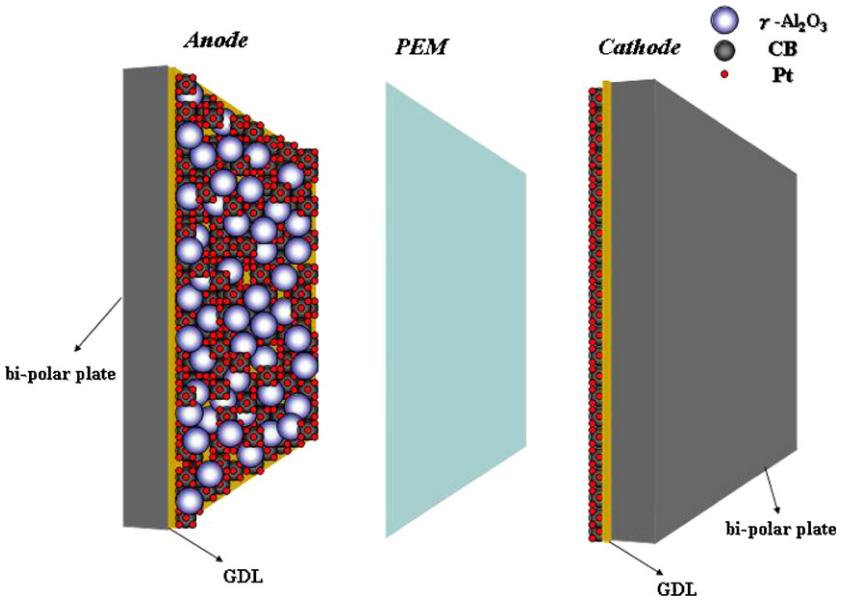

Fig. 1. A schematic diagram of the γ-alumina added membrane electrode assembly.

electrodes under low-humidity conditions [14–27]. Some studies have synthesized composite membranes by combining solid acids and heteropolyacids such as sulfonated ZrO_2, phosphotungstic acid, and molydophosphoric acid, to increase the acid sites that promote local migration and improve the proton conductivity [28,29].

In PEMFC, the catalyst layer sandwiched between the gas diffusion layer and Nafion® membrane often contains Nafion® to ensure the proton continuity and extend the three-phase boundary. Under low-humidity conditions, the Nafion® binder in the catalyst layer is prone to loss of water content in the electrodes due to its hydrophobic characteristic, resulting in reduction of proton conductivity and degradation in cell performance. Therefore, a composite catalyst layer consisting of hygroscopic particles that maintain the proton conductivity in the catalyst layer under low-humidity is needed. Several researches have proposed to prepare the composite catalyst layer by adding hygroscopic SiO_2 particles into the layer to improve the wettability and performance of the membrane electrode assembly (MEA) at low-humidity conditions [30,31].

Being one of the widely used inorganic materials in chemical industry, alumina is commonly used as adsorbents, catalysts, catalyst support and surface coatings in various industrial fields [32]. The aim of this study is to explore the feasibility of adding hygroscopic γ-alumina particles into the anode catalyst layer to improve the wettability of the anode under low-humidity conditions by utilizing the Lewis acid sites on the surface of γ-alumina that can attract the hydroxyl group of the water molecular [33–35]. High BET surface area γ-alumina particles were added to the anode catalyst layer by using an ultrasonic technique. The wettability of the anode electrode was determined by the sessile drop method. The cell performance was evaluated by an electrochemical polarization method under different anode humidifier temperatures with the cell temperature set at 65 °C and the cathode humidifier temperature at 55 °C.

2. Experimental

2.1. Preparation of high BET surface area γ-alumina particles

The γ-alumina particles were synthesized by a three-step sol–gel process (hydrolysis, condensation, calcination) in basic medium using aluminum isopropoxide (AIP) as the precursor. First, the hydrolysis process of AIP was carried out at ambient conditions for 1 h, in which the molar ratio of AIP:H_2O was 1:100, and then the PH value of the mixture was adjusted to 10. Subsequently, the temperature was raised to 80 °C for the condensation process of aluminum sol through evaporation of the solvent, before drying at 100 °C for 10 h. Finally, the as-synthesized aluminum hydroxide powders were calcined at 500 °C for 6 h to form γ-alumina particles via a phase transformation process.

2.2. Preparation of membrane electrode assembly

A 20 wt% Pt/C catalyst, 5 wt% Nafion® solution (Dupont®), the above-mentioned γ-alumina particles and alcohol (98%, Aldrich) were mixed by using an ultrasonator for 1 h, and then sprayed onto commercial hydrophobic carbon clothes (Beam associate Co., Ltd) and dried at 60 °C for 3 h, which served as the anode electrode. The cathode electrode was prepared by a similar method, but without the addition of γ-alumina particles. A Nafion® 112 membrane (Dupont®) was pretreated with 5 wt% H_2O_2 (Aldrich), deionized water, 1.0 M H_2SO_4 (Aldrich) and deionized water at 80 °C for 1 h, sequentially. Thereafter, the Nafion® 112 membrane (Dupont®) was sandwiched between the anode and the cathode before being hot-pressed under 100 kg f cm^{-2} at 130 °C for 2 min. A schematic diagram of the MEA structure is shown in Fig. 1. The Pt loading at both anode and cathode was 0.6 mg cm^{-2} and the effective area of the MEA was 5 cm^2. Table 1 gives the compositions of the MEAs.

2.3. Characterization of γ-alumina particles and Pt/C/γ-alumina catalyst ink

A wide angle X-ray diffraction (XRD) study of the γ-alumina particles was performed by a MAC MXP III X-ray diffractometer using Cu Kα radiation, and the diffraction peaks were compared with the JCPDS data file. The pore size distribution and Brunauer–Emmett–Teller (BET) surface area of the γ-alumina particles were determined by a Micromeritics ASAP 2010 system. Morphology of the γ-alumina particles and the catalyst ink was investigated by a JEOL 5400 scanning electron microscope (SEM).

Table 1
Compositions of membrane electrode assemblies

MEA	Weight fraction based on Pt/C			Electrode with γ-alumina addition
	20 wt% Pt/C	γ-Alumina	5 wt% Nafion® solution	
AL0	1	0	3	None
AL10A	1	0.1	3.3	Anode
AL20A	1	0.2	3.6	Anode
AL40A	1	0.4	4.2	Anode
AL40C	1	0.4	4.2	Cathode

AL40A stands for 40% γ-alumina particles added in the anode catalyst layer. AL40C stands for 40% γ-alumina particles added in the cathode catalyst layer.

Electrical resistance of the catalyst ink was measured by a Keithley 6517A powder electrical resistance instrument. The sessile drop method using a Fat 200 contact angle system was used to measure the contact angle of water on a solid surface. Catalyst ink was sprayed onto one side of commercial hydrophobic carbon clothes, and then dried at 60 °C for 30 min. Each sample was measured at different locations five times and the average value of water contact angle was calculated.

2.4. Measurement of polarization curves

A fuel cell test station, Beam 100 from Beam associate Co., Ltd, was used to measure the polarization curves of a 5 cm^2 single cell with the serpentine flow pattern as shown in Fig. 2. Hydrogen and oxygen served as fuels and the gas flow rate (100 cm^3 min^{-1}) for hydrogen and oxygen was kept constant during measurement. Different anode humidifier temperatures at 25, 35, 45, and 55 °C were designed to investigate the influence of anode humidification on cell performance. The cell temperature and the cathode humidifier were fixed at 65 and 55 °C, respectively. The polarization measurement was conducted at ambient conditions.

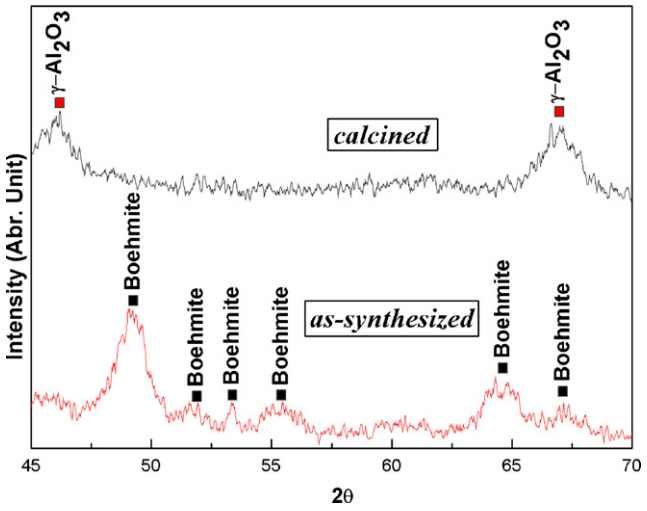

Fig. 3. Wide angle X-ray diffraction spectra of the as-synthesized aluminum hydroxide and the calcined powders.

3. Results and discussion

3.1. Characterization of γ-alumina particles and Pt/C/γ-alumina catalyst ink

Fig. 3 displays the wide angle X-ray diffraction (XRD) spectra of the as-synthesized aluminum hydroxide powders and that calcined at 500 °C. It reveals that a chemical structural transformation has occurred upon the calcination process. The structure of the as-synthesized aluminum hydroxide is in accord with that of boehimite (AlOOH) and the calcined powder corresponds to the crystalline phase of γ-alumina (γ-Al_2O_3), by comparing the 2θ values of the diffraction peaks with those of the standard compounds

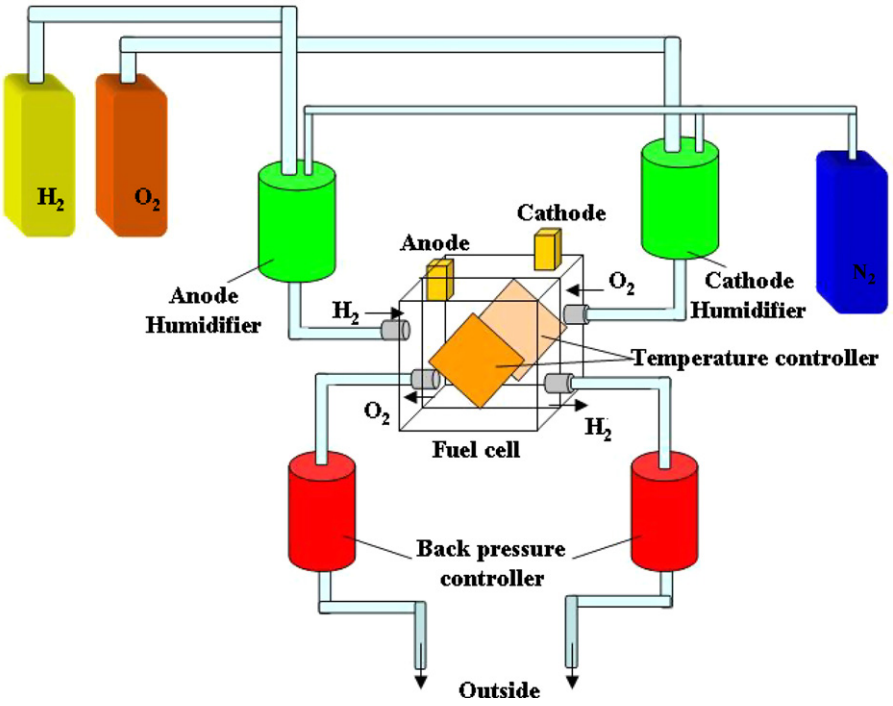

Fig. 2. A schematic diagram of the polarization testing system.

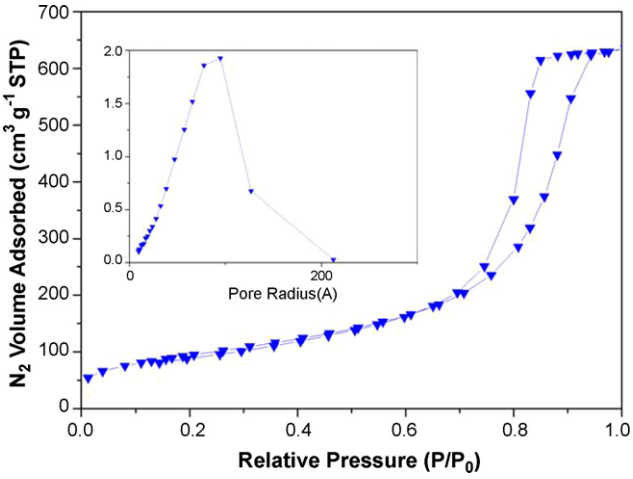

Fig. 4. N_2 adsorption isotherm and pore size distribution of the γ-alumina particles.

reported in the JCPDS data file. The chemical reaction for the transformation of boehimite is as follows [36]:

$$Al^{3+} + 3H_2O \leftrightarrow AlOOH(s) + 3H^+ \quad \log K = -8.58$$

Fig. 4 presents the nitrogen adsorption isotherm and the pore size distribution (inset) of γ-alumina particles. The shape of the isotherm curve is similar to that of the classical type IV of Brunauer isothermal adsorption curve (IUPAC classification), typically characterized to be the mesoporous materials. A hysteresis loop occurred at high relative pressure (P/P_0 = 0.7–0.9). The BET surface area of the γ-alumina synthesized by this sol–gel procedure is 442 $m^2\ g^{-1}$ and the mean pore diameter is 9 nm, which is in the range of the mesoporous materials. The field emission SEM micrograph in Fig. 5 shows the sphere-like microstructure of the γ-alumina particles.

The Pt/C/γ-alumina catalyst ink consists of Pt/C catalyst, Nafion® solution, alcohol and γ-alumina particles, as listed in Table 1. The ink was analyzed by wide angle X-ray diffraction (XRD) and field emission scanning electron microscopy (SEM) to understand its microstructure and the distribution of γ-alumina particles therein. Fig. 6 shows the wide angle X-ray diffraction (XRD) spectra of the Pt/C catalyst ink and the Pt/C/γ-alumina catalyst ink. The diffraction peaks clearly demonstrates the presence of Pt, Carbon black and γ-alumina at the 2θ values of 31.8°, 39.3°, and 60.5°. Fig. 7

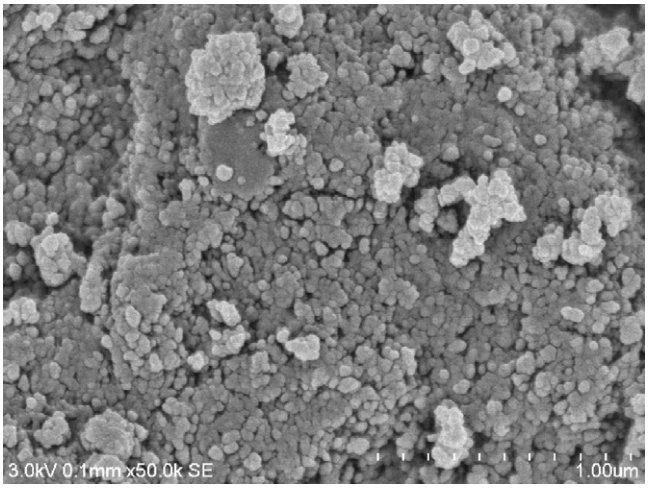

Fig. 5. Field emission SEM micrograph of the γ-alumina particles.

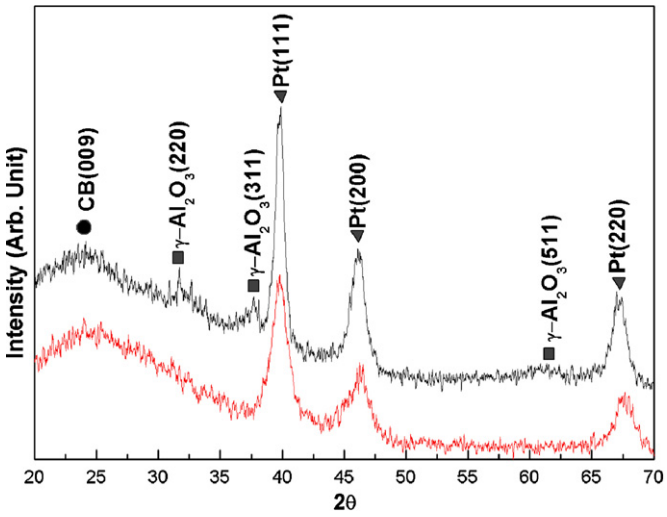

Fig. 6. Wide angle X-ray diffraction spectra of the Pt/C catalyst and Pt/C/γ-alumina catalyst ink.

gives the field emission SEM images of the Pt/C/γ-alumina catalyst inks with 10%, 20% and 40% of γ-alumina addition. These images indicate that the γ-alumina particles are well-dispersed in the catalyst layer, even for the 40% γ-alumina addition. Table 2 presents the electrical measurement results, in which the electrical resistance of the Pt/C/γ-alumina catalyst ink with various amounts of γ-alumina addition is given. Specifically, the electrical resistance of the Pt/C/γ-alumina catalyst ink with 20% γ-alumina addition is about two-order of magnitude higher than that of the Pt/C/γ-alumina catalyst ink with 10% γ-alumina addition. The later is nearly three-order of magnitude higher than that without γ-alumina addition. This huge change in electrical resistance could cause a significant impact on the cell performance. In summary, the electrical resistance of the catalyst ink increases dramatically with the amount of added γ-alumina.

3.2. Water contact angle of the catalyst layer

The hydrophilic characteristics of the Pt/C/γ-alumina catalyst layer in the membrane electrode assembly (MEA) were further investigated by using the sessile drop method. Fig. 8 presents the water droplet images on each catalyst layer with various amounts of added γ-alumina. The water contact angles of the catalyst layer with various amounts of γ-alumina 0%, 10%, 20% and 40% are 136°, 109°, 79° and 0°, respectively. In other words, the water contact angle decreases as the amount of γ-alumina increases. The wettability of γ-alumina-added catalyst layer differs obviously from that of the Pt/C catalyst layer and is strongly related to the amount of added γ-alumina. A comparison with the results of adding SiO_2 particles into the catalyst layer [30] indicates that γ-alumina exhibits better wettability than SiO_2 for the same amount of addition.

3.3. Single cell polarization test

3.3.1. Adding γ-alumina to the cathode catalyst layer

It is known that when the temperature of the cathode humidifier is too high, excess water could be produced in the cathode and then water flooding occurs. Under flooding conditions, water accumulates at the channels of bipolar plate, the gas diffusion layer and the catalyst layer, preventing the oxygen from accessing the catalyst layer, and resulting in degradation in the cell performance. Fig. 9, polarization curves of the MEAs measured at the anode and cathode humidifier temperature 55 °C and the cell temperature 65 °C,

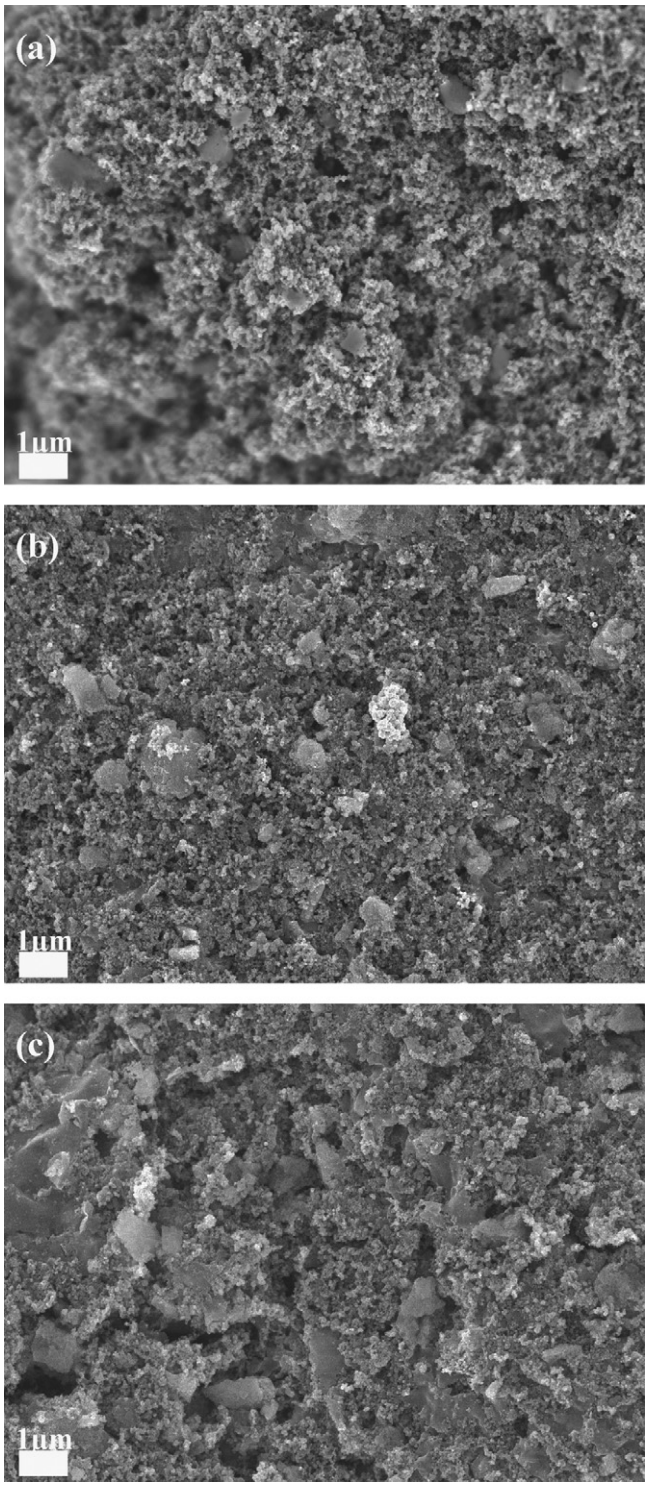

Fig. 7. Field emission SEM micrographs of the Pt/C/γ-alumina catalyst ink with different γ-alumina addition (a) 10%, (b) 20%, (c) 40%.

Table 2
Electrical properties of the Pt/C/γ-alumina catalyst ink

γ-Alumina content (%)	Electrical resistance (Ω)	Electrical conductivity (S cm^{-1})
0	6.91×10^{5}	1.449×10^{-6}
10	2.31×10^{8}	2.165×10^{-9}
20	1.2×10^{10}	4.167×10^{-11}
40	2.1×10^{11}	2.381×10^{-12}

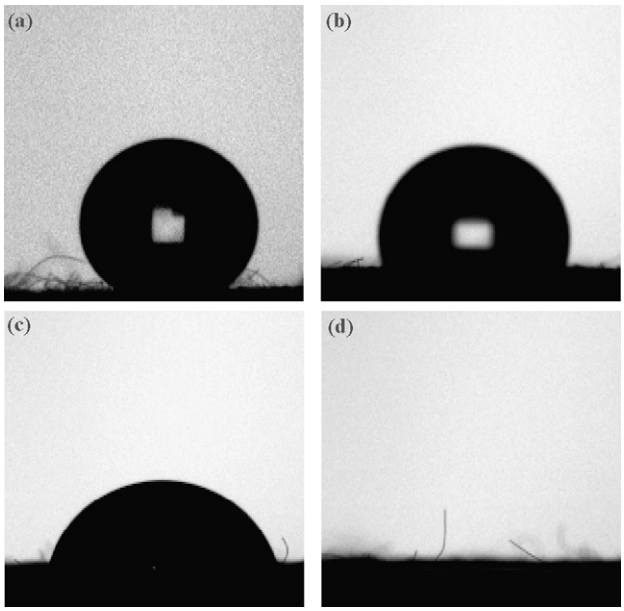

Fig. 8. The results of contact angle measurement using water droplets on the Pt/C catalyst layer with (a) 0%, (b) 10%, (c) 20%, (d) 40% γ-alumina additions.

indicates a considerable decline in the current density of the MEA with 40% γ-alumina addition in the cathode catalyst layer. The MEA made of AL40C catalyst ink containing 40% hygroscopic γ-alumina particles in the cathode catalyst layer gives rise to severe water flooding, compared with the MEA without γ-alumina addition. In this case, water flooding occurred not only in the catalyst layer but also in the gas diffusion layer and the channels of the bipolar plate. This result demonstrates that adding hygroscopic γ-alumina particles to the cathode catalyst layer is detrimental. However, it suggests that the hygroscopic γ-alumina particles could be utilized to improve the wettability of the anode catalyst layer as discussed below.

3.3.2. *Adding γ-alumina to the anode catalyst layer*

A polarization test with various amounts of γ-alumina added to the anode catalyst layer was carried out at different temperatures of the anode humidifier with the temperature of single cell and the cathode humidifier fixed. The cell performance was evaluated

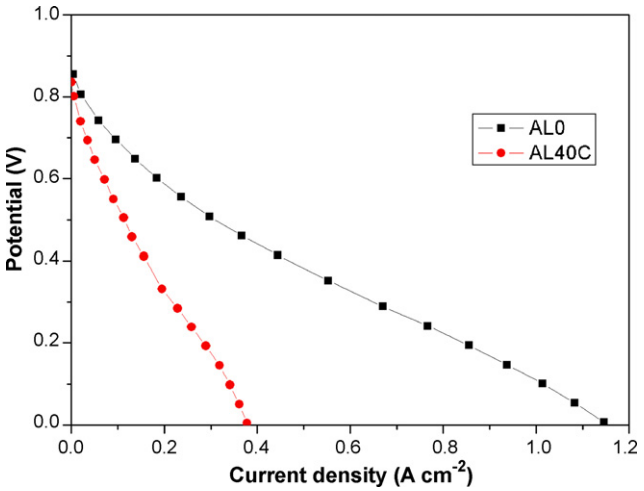

Fig. 9. Polarization curves of MEAs measured at the anode and cathode humidifier temperature 55 °C and the cell temperature 65 °C, respectively.

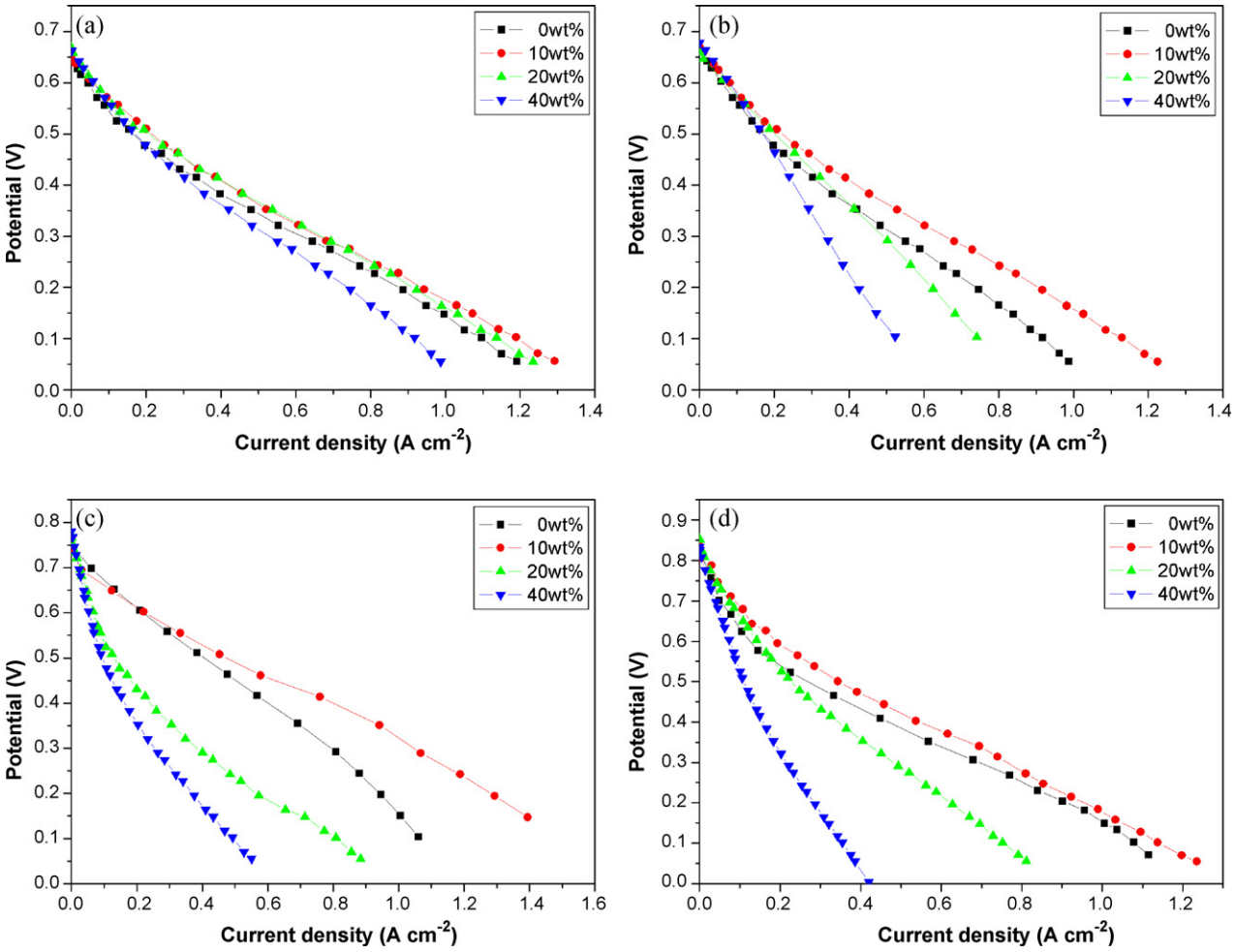

Fig. 10. Polarization curves of the MEAs measured at different anode humidifier temperatures (a) 25 °C, (b) 35 °C, (c) 45 °C, (d) 55 °C with the cell temperature at 65 °C and the temperature of cathode humidifier at 55 °C, respectively.

on the basis of voltage versus current density curves as shown in Fig. 10.

Fig. 10(a) plots the polarization curves for which the temperature of the anode humidifier is 25 °C. It can be seen that the order of the current density at the cell voltage 0.1 V is AL10A > AL20A > AL0 > AL40A. This result proves the feasibility of improving low-humidity performance of MEAs by adding γ-alumina particles into the anode catalyst layer because the wettability of the anode is improved. It is also noted that the current density of the MEA AL20A at 0.1 V is lower than that of AL10A, but higher than that of AL0. Similarly, the current density of MEA AL40A at 0.1 V is much lower than that of AL0 because of the high anode electrical resistance. In general, if the improvement of cell performance is due only to the uptake of water from an external humidifier, then the current density would not change noticeably [30]. However, a considerable difference in the current density was observed, indicating a back diffusion has occurred in the anode. Consequently, γ-alumina particles have assisted the adsorption of water by simultaneous external humidification and back diffusion.

Fig. 10(b) gives the polarization curves for which the temperature of the anode humidifier is 35 °C. The current density of MEAs at the cell voltage of 0.1 V follows the sequence AL10A > AL0 > AL20A > AL40A. The current density of the MEA AL20A exceeds that of AL0 in the high cell voltage range (>0.3 V), but is lower than that of AL0 at low cell voltage (<0.3 V), very likely due to the excess water adsorbed by the γ-alumina particles, causing flooding in the anode. Fig. 10(c) shows the polarization curve of the cell at anode humidifier temperature 45 °C. The current density of MEAs at 0.1 V follows similar order as that of anode humidifier temperature 35 °C, except that the current density of the MEA AL20A is always lower than that of AL0 over the entire range of cell voltages. Fig. 10(d) plots the polarization curve when the temperature of the anode humidifier is 55 °C. The current density of the MEAs at the cell voltage of 0.1 V follows the order AL10A > AL0 > AL20A > AL40A, but the difference in current density between AL10A and AL0 is smaller than those at other anode humidifier temperatures. Since the wettability of the anode was better at this temperature, adding γ-alumina particles into the anode catalyst layer seems useless. The current density of the MEA AL40A was the lowest at each temperature of the anode humidifier, and the value decreased significantly as the temperature increased because of the high electrical resistance and the absorption by γ-alumina particles of excess water that accumulated in the channel of the anode bipolar plate.

The cell performance is determined by a competition mechanism between the wettability of the catalyst layer in the MEA and internal resistance of the cell. Theoretically, the dryer anode gas needs a higher amount of γ-alumina addition to retain its optimum hydration level. However, as given in Table 2, the electrical resistance of the anode catalyst ink with 20% γ-alumina addition is about two-order of magnitude higher than that of the 10% γ-alumina addition. In contrast, the saturation water vapor pressure at each 10 °C increment of temperature is only increased by less than two

Table 3
Saturation vapor pressure of water

Temperature (°C)	Pressure (Torr)
25	23.8
35	42.2
45	71.9
55	118.0

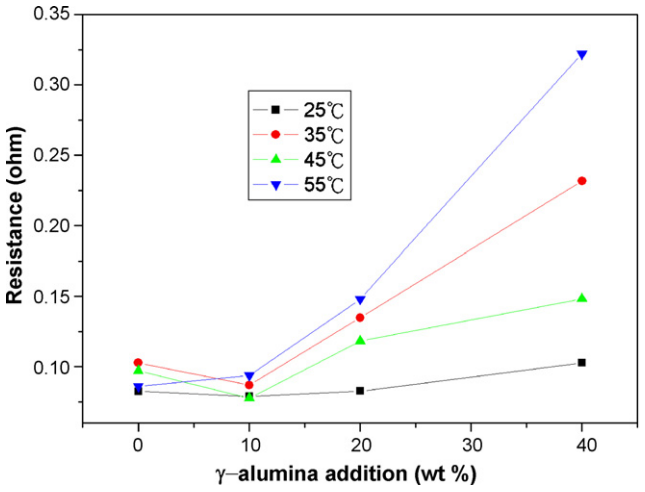

Fig. 11. The internal resistance versus γ-alumina addition curves at different anode humidifier temperatures with the cell temperature at 65 °C and the cathode humidifier temperature at 55 °C.

times, as given in Table 3. Therefore, it can be concluded that the effect of electrical resistance of the catalyst ink with γ-alumina addition is apparently surpassed that of the anode humidifier temperature. Nevertheless, it is known that the electrical resistance of the catalyst ink might be differed from the internal resistance of the single cell, which can be calculated from the polarization curves. For further understanding, the empirical equations from Tu et al. [37] were adopted to estimate the internal resistance of the single cell from the polarization curves, and the result is plotted in Fig. 11. As can be seen, the internal resistance increases considerably with theγ-alumina addition from 10 to 40 wt%, in particular, at high anode humidifier temperatures, e.g. 45 and 55 °C. The internal resistances with 10 wt% γ-alumina addition reach the lowest value at the anode humidifier temperatures of 25, 35 and 45 °C due to the proper hydration level was achieved by adding γ-alumina in the catalyst layers to reduce the internal resistance. This result further confirms that the amount of γ-alumina addition is directly related to the internal resistance, which plays an important role in the control of cell performance. In addition, it is noted that the trend of the internal resistance with γ-alumina addition is quite similar to that of the electrical resistance of the catalyst ink, except that the catalyst ink without γ-alumina addition always has the lowest electrical resistance.

4. Conclusion

Hygroscopic γ-alumina particles with a BET surface area of 442 $m^2 g^{-1}$ and an average pore diameter of 9 nm were synthesized by a three-step sol–gel process. These γ-alumina particles were added, up to 40%, to the catalyst layer of MEAS by utilizing an ultrasonic technique. The water contact angle of the catalyst layer with added γ-alumina was measured by a sessile drop method at ambient conditions. It was observed that as the amount of added γ-alumina was increased, the water contact angle became smaller and the wettability improved. Among all the specimens in which γ-alumina particles were added to the anode catalyst layer, the MEA with 10% γ-alumina addition exhibits the highest current density at different anode humidifier temperatures ranging from 25 to 55 °C. Since the cell performance is determined by a competition mechanism between wettability and the variation of electrical resistance caused by upon γ-alumina addition, it is found that the optimum concentration of γ-alumina in the Pt/C catalyst layer is about 10%. In addition, it is noticed that better wettability of the MEA facilitates the adsorption of water to the anode by back diffusion.

Acknowledgments

The authors would like to thank the National Science Council of Taiwan, for financially supporting this research under Contract No. NSC-96-2623-7-005-002-ET and NSC-95-ET-7-005-003-ET. Partially support of this research by the ministry of education under ATU program is gratefully acknowledged.

References

[1] D.O.J. Murphy, G.D. Hitchens, D.J. Manko, J. Power Sources 47 (1994) 353.
[2] K.B. Prater, J. Power Sources 61 (1996) 105.
[3] M.L. Perry, T.F. Fuller, J. Electrochem. Soc. 149 (2002) S59.
[4] P. Sridhar, R. Perumal, N. Rajalakshmi, M. Raja, K.S. Dhathathretan, J. Power Sources 101 (2001) 72.
[5] S. Ren, G. Sun, C. Li, S. Song, Q. Xin, X. Yang, J. Power Sources 157 (2006) 724.
[6] A. Sacca, A. Carbone, E. Passalacqua, A. D'Epifanio, S. Licoccia, E. Traversa, E. Sala, F. Traini, R. Ornelas, J. Power Sources 152 (2005) 16.
[7] R. Eckl, W. Zehtner, C. Leu, U. Wagner, J. Power Sources 138 (2004) 137.
[8] Y. Qiangu, T. Hossein, W. Junxiao, J. Power Sources 158 (2006) 316.
[9] F.B. Weng, A. Su, C.Y. Hsu, C.Y. Lee, J. Power Sources 157 (2006) 674.
[10] M.M. Saleh, T. Okajuma, M. Hayase, F. Kitamura, T. Ohsaka, J. Power Sources 164 (2007) 503.
[11] Z. Hou, B. Yi, H. Yu, Z. Lin, H. Zhang, J. Power Sources 123 (2003) 116.
[12] T. Vidaković, M. Christov, K. Sundmacher, J. Electrochim. Acta 52 (2007) 5606.
[13] H. Xu, Y. Song, H.R. Kunz, J.M. Fenton, J. Power Sources 159 (2006) 979.
[14] S.H. Kwak, T.H. Tang, C.S. Kim, K.H. Yoon, J. Power Sources 118 (2003) 200.
[15] F. Liu, B. Yi, D. Xing, J. Yu, Z. Hou, Y. Fu, J. Power Sources 124 (2003) 81.
[16] Z.G. Shao, P. Joghee, I.M. Hsing, J. Membr. Sci. 229 (2004) 43.
[17] N.H. Jalani, K. Dunn, R. Datta, Electrochim. Acta 51 (3) (2005) 553.
[18] F. Bauer, M. Willert-Porada, J. Power Sources 145 (2005) 101.
[19] S.Y. Chen, C.C. Han, C.H. Tsai, J. Huang, Y.W. Cheng-Yang, J. Power Sources 171 (2007) 363.
[20] G. Alberti, M. Casciola, Annu. Rev. Mater. Res. 33 (2003) 129.
[21] K.A. Manuritz, Mater. Sci. Eng. C 6 (1998) 121.
[22] B. Kumar, J.P. Fellner, J. Power Sources 123 (2003) 132.
[23] K.T. Adjemian, S.J. Lee, S. Srinivasan, J. Benziger, A.B. Bocarsly, J. Electrochem. Soc. 149 (2002) A256–A261.
[24] V. Tricoli, F. Nannetti, Electrochim. Acta 48 (2003) 2625.
[25] E. Chalkova, M.B. Pague, M.V. Fedkin, D.J. Wesolowski, S.N. Lvova, J. Electrochem. Soc. 152 (6) (2005) A1035.
[26] V.D. Noto, R. Gliubizzi, E. Negro, M. Vittadello, G. Pace, Electrochim. Acta 53 (2007) 1618.
[27] Y. Tominaga, I. Hong, S. Asai, M. Sumita, J. Power Sources 171 (2007) 530.
[28] F. Croce, L. Settimi, B. Scrosati, Electrochem. Commun. 8 (2006) 364.
[29] Y.S. Kim, F. Wang, M. Hickner, T.A. Zawodzinski, J.E. McGrath, J. Membr. Sci. 212 (2003) 263.
[30] U.H. Jung, K.T. Park, E.H. Park, S.H. Kim, J. Power Sources 159 (2006) 529.
[31] S. Vengatesan, H.J. Kim, S.Y. Lee, E. Cho, H.Y. Ha, I.H. Oh, S.A. Hong, T.H. Lim, Int. J. Hydrogen Energy 33 (2008) 171.
[32] Z.X. Sun, T.T. Zheng, Q.B. Bo, M. Du, W. Forsling, J. Colloid Interface Sci. 319 (2008) 247.
[33] B.H. Milosavljevic, J.K. Thomas, J. Phys. Chem. B 107 (2003) 11907.
[34] M. Digne, P. Sautet, P. Raybaud, P. Euzen, H. Toulhoat, J. Catal. 211 (2002) 1.
[35] B. Hu, I.D. Gay, J. Phys. Chem. B 105 (2001) 217.
[36] R.M. Smith, A.E. Martell, Inorganic Complexes, in: Critical Stability Constants, vol. 4, Plenum, New York, 1976.
[37] H.C. Tu, Y.Y. Wang, C.C. Wan, K.L. Hsueh, J. Power Sources 159 (2006) 1105.